

Testing the Pressure-confined Ly α Cloud Model

ARIF BABUL¹ & GERARD M. WILLIGER²

¹Canadian Institute for Theoretical Astrophysics, Toronto, Canada

²Cerro Tololo Inter-American Observatory, La Serena, Chile

Introduction: The Ly α absorption line forest, seen in quasar spectra, is generally interpreted as being due to cosmologically distributed “clouds” of primordial gas. Analyses of the observations (*e.g.* Rauch *et al.* 1992) reveal that the number distribution can be described by power laws: $dN/dz \propto (1+z)^\gamma$ and $dN/dN_{HI} \propto N_{HI}^{-\beta}$, where N_{HI} is the HI column density. The typical values for power law indices range between $2 \lesssim \gamma \lesssim 2.6$ and $1.7 \lesssim \beta \lesssim 1.9$. One model postulates that the Ly α clouds are optically thin entities, photoionized by the background UV flux, $J_\nu \propto (1+z)^j$, and confined by an adiabatically evolving intercloud medium (ICM): $P(z) \propto (1+z)^5$. Analytic studies of this model suggest that the ensuing Ly α line statistics can account for the observations (in particular, the dN/dz and the dN/dN_{HI} distributions) if the cloud mass spectrum is a power law $dN/dM \propto M^{-\delta}$, $\delta \approx 1.9$, and $j \approx 4$ (*c.f.* Ikeuchi & Ostriker 1986, IO). One of the simplifying assumptions incorporated into these studies is the existence of a large mass range for the clouds at all epochs, the validity of which is questionable.

Simulations: We investigate the pressure-confined model using a 1-D spherically symmetric hydrodynamical code to simulate cloud evolution over the epoch $1.8 \leq z \leq 6$. This enables us to relax many of the assumptions incorporated in the analytic studies. We only consider clouds with masses $2.75 \leq \log(M/M_\odot) \leq 9.25$. Clouds with larger masses are Jeans unstable and tend to collapse; they are not “pressure-confined”. The lower mass limit is chosen to ensure all clouds that can produce absorption features with equivalent widths $W_r \geq 0.2\text{\AA}$ over the epoch $1.8 \leq z \leq 3.6$ are considered. We calculate Voigt profiles from the model clouds at varying impact parameters and use the resulting absorption features to determine line-profile parameters (*e.g.* N_{HI} , the rest-frame equivalent width W_r , and the Doppler parameter b). We construct synthetic samples of lines subject to similar selection criteria used to define a sample of ~ 400 observed lines (*i.e.* $W_r \geq 0.2\text{\AA}$). In this sense, the present study is unique: past theoretical studies have relied on column density thresholds. N_{HI} , however, is a fitted parameter and is sometimes subject to large uncertainties. Line widths have been traditionally used to define observational samples as they are directly measurable. We compare the synthetic dN/dW_r , dN/dN_{HI} and dN/dz distributions against the observed trends. The synthetic results are normalized by demanding that the number of clouds with $W_r \geq 0.2\text{\AA}$ be the same as observed. Apart from studying the properties of clouds immersed in $j = 4$ UV background, we also consider the possibility that the UV background is constant at the epoch of interest. For more details, see Williger & Babul (1992; WB).

Results: The redshift-integrated dN/dW_r distributions for $j = 0, 4$ ($\delta = 1.90$) are shown in Figure 1. Clearly, there is a shortage of model lines with $W_r > 0.3\text{\AA}$, in comparison with the observations. The result is partly due to the fact that $\langle b \rangle \approx 22 \text{ km s}^{-1}$ for simulated pressure-confined clouds (with a dispersion of approx. 1 km s^{-1}) — *i.e.* b is due to thermal velocities — while $\langle b \rangle \approx 35 \text{ km s}^{-1}$ for the observed lines (with a dispersion of approx. 15 km s^{-1}). The lower b for the simulated clouds implies that these clouds require larger column densities than those associated with the observed lines in order to account for the observed dN/dW_r distribution. The imposition of the upper mass limit for the pressure-confined clouds, however, restricts the column density range of the simulated clouds.

The dN/dN_{HI} distributions for the simulated and the observed clouds in the redshift range $2.6 \leq z \leq 2.8$ (Figure 2) shows that although the two are consistent with each other for $\log(N_{HI}) \lesssim 15.2$, there are fewer model clouds with N_{HI} larger than observed. Note that the shortage is more severe for the $j = 4$ case as the UV background at $z \approx 2.7$ is more intense than in the $j = 0$ case and therefore the clouds are more highly ionized. We also show the “analytic” dN/dN_{HI} , computed using the simple homologously-expanding pressure-confined cloud model of IO and the prescription of WB (*e.g.* we explicitly take into account the upper mass limit). This distribution cuts off at even a lower N_{HI} than the synthetic distribution; the simulations reveal that the more massive clouds tend not to expand homologously and, consequently, develop non-uniform density profiles. Self-gravity also retards their expansion.

In Figure 3, we show the observed and the synthetic dN/dz distributions for clouds with $W_r \geq 0.2\text{\AA}$; the dN/dz distribution for a subset of clouds with $W_r \geq 0.3\text{\AA}$ is shown in Figure 4. For $W_r \geq 0.2\text{\AA}$ sample, the synthetic results match the observations well. Neither the normalization (reflecting the discrepancy in

the dN/dW_r distributions) nor the slope of the synthetic dN/dz (the number of pressure-confined clouds decreases much too rapidly at low redshifts) matches the observations for the subset with $W_r \geq 0.3\text{\AA}$. The rapid decline in clouds with large equivalent widths towards lower redshifts is, once again, due to the upper mass limit for the clouds.

Conclusions: As a result of an upper limit to the mass of pressure-confined clouds and the “thermal” Doppler parameters, the equivalent width and column density distributions for spherical, pressure-confined clouds with a power-law mass spectrum fail to account for the observations. The upper mass limit is determined by nature of the evolution of both the ICM pressure and the UV background; in order to achieve an acceptable fit to the data, we require the ICM pressure to decrease as $P(z) \propto (1+z)^p$, $p \gtrsim 5.8$ (WB). This is difficult to justify physically. Aspherical clouds, on the other hand, may allow the pressure-confined model to remain viable.

References: Ikeuchi, S. & Ostriker, J.P. 1986, *Astrophys. J.*, 301, 522.

Rauch, M., et al. 1992 *Astrophys. J.*, 390, 387.

Williger, G.M. & Babul, A., 1992. *submitted to Astrophys. J.*

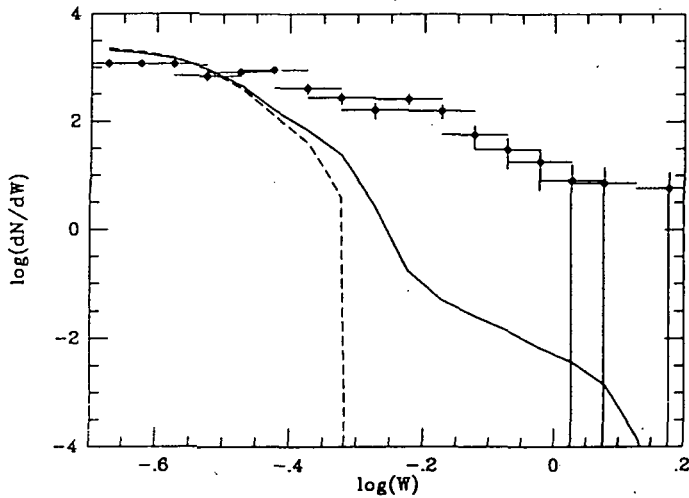


Fig. 1. dN/dW_r of the observed clouds vs. the z -integrated distribution of the model clouds. The $j = 0, 4$ cases for $\delta = 1.90$ are shown by solid, dashed lines respectively. The error bars indicate bin widths and 1σ errors for the observations.

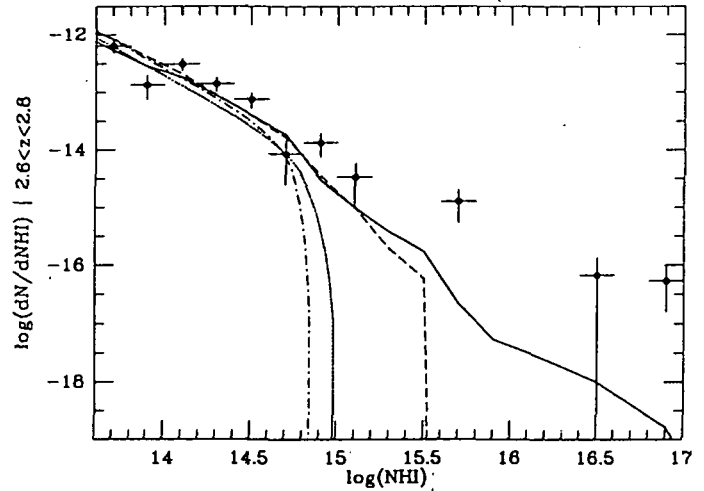
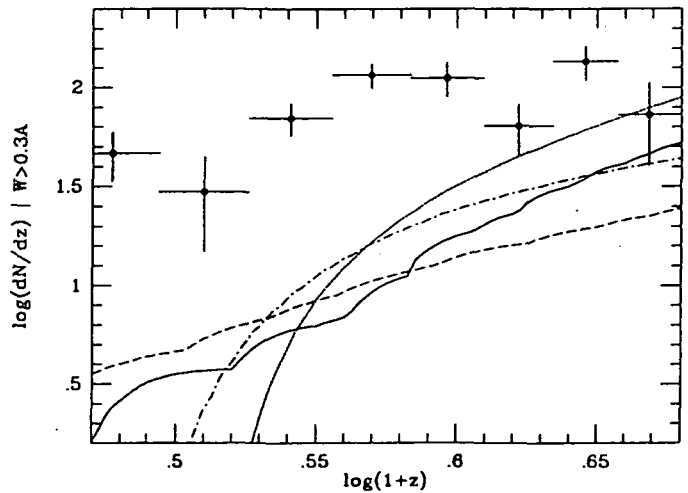
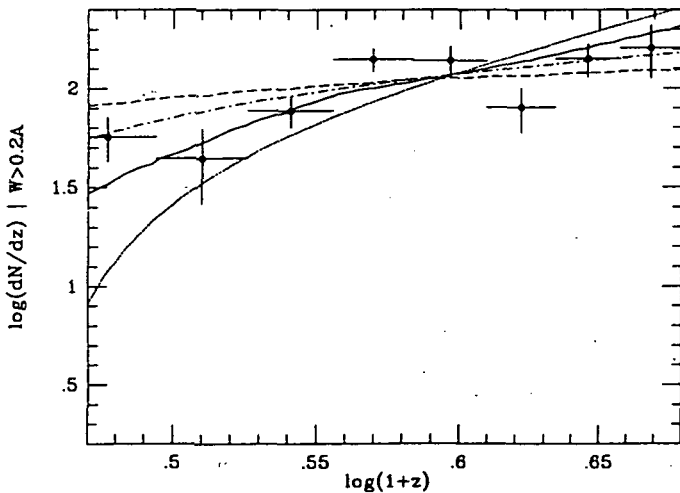


Fig. 2. Column density distribution of the observed clouds vs. models in the redshift range $2.6 < z < 2.8$. The various curves correspond to various analytic and synthetic results: $j = 0/j = 4$ synthetic (solid/dashed); $j = 0/j = 4$ analytic (dotted/dot-dashed). At high N_{HI} , the synthetic curves steepen before an abrupt cutoff. The cutoff is even lower for the analytic models.



Figs. 3-4. The observed vs. model redshift distribution of Ly α clouds with $W_r \geq 0.2\text{\AA}$ (Fig. 3) and $W_r \geq 0.3\text{\AA}$ (Fig. 4). The various curves correspond to various analytic and synthetic results: $j = 0/j = 4$ synthetic (solid/dashed); $j = 0/j = 4$ analytic (dotted/dot-dashed). Although the synthetic curves fit the data for $W_r \geq 0.2\text{\AA}$, there are significant discrepancies in the slope and the normalization for $W_r \geq 0.3\text{\AA}$. The analytic fits are worse, except for $j = 4$, $W_r \geq 0.2\text{\AA}$.